ISSN 1063-7710, Acoustical Physics, 2019, Vol. 65, No. 1, pp. 14–22. © Pleiades Publishing, Ltd., 2019.

CLASSICAL PROBLEMS OF LINEAR ACOUSTICS AND WAVE THEORY

Theoretical and Numerical Studies on in vacuo Structural Admittance of an Infinite, Coated Cylindrical Shell[1]

Fulin Zhou[a, b, *], Bin Wang[a, b, **], Jun Fan[a, b, *], and Zilong Peng[a, b, c, ****]**

[a]*Collaborative Innovation Center for Advanced Ship and Deep-Sea Exploration, Shanghai Jiao Tong University, Shanghai, 200240 China*

[b]*State Key Laboratory of Ocean Engineering, Shanghai Jiao Tong University, Shanghai, 200240 China*

[c]*School of Energy and Power Engineering, Jiangsu University of Science and Technology, Zhenjiang, 212003 China*

**e-mail: zhoufulin@sjtu.edu.cn*

***e-mail: bin_wang@sjtu.edu.cn*

****e-mail: fanjun@sjtu.edu.cn*

*****e-mail: zlp_just@sina.com*

Received May 29, 2018; Revised September 12, 2018; Accepted October 30, 2018

Abstract—Studying the interaction of sound with a coated cylindrical shell immersed in water is essential for improving existing underwater target detection and classification algorithms. According to the impedance theory of sound scattering, in vacuo structural admittance describes the relationship between the sonar-induced forces and the resulting vibration on the surface, which can be used to solve the problem of the acoustic scattering and radiation. In this work, we investigate numerically and theoretically the structural admittance of a coated cylindrical shell. Analytical expressions of the structural admittance are derived for different external forces: a plane acoustic wave, a normal point force, and a random noise field. The structural admittance is also numerically evaluated. The results show that the structural admittance is independent of exterior medium and fluid loading. According to the impedance theory of sound scattering, the scattered field of a coated cylindrical shell is calculated by combining the structural-, acoustic-, and internal-admittance matrices. Because of the non-local property of structural surface admittance, we build an algebraic model of a coated object by nonlinear curve fitting and study a local approximation of the structural admittance. We also find that simplifying the large matrices is useful for research on structural vibrations. Thus, this work presents a systematic study of the acoustic scattering characteristics of structural admittance of an infinite, coated cylindrical shell.

Keywords: acoustic scattering, coated cylindrical shell, structural admittance

DOI: 10.1134/S1063771019010184

INTRODUCTION

The impedance theory of sound scattering formulated by Bobrovnitskiĭ [1, 2] brings a new approach to the study the underwater acoustic scattering characteristics of a coated submarine, which is a vital concern. The scattering problem is described by the structural, the acoustic, and the internal impedances. The structural impedance characterizes the response of the elastic body in vacuum and so, depends only on the object's structural parameters. The acoustic and the internal impedances depend only on the body geometry and the fluid properties. Numerical methods, such as the finite element method (FEM) and the boundary element method, can be used to find these impedances [3–5]. The Bobrovnitskiĭ theory, therefore, gives a concise, clear physical description of the problem and facilitates the mechanism analysis thereof. It also has been used to optimize surface coatings to reduce the scattered field signatures [6–8].

By considering the key role of the structural impedance in solving the scattering problem [9], Rakotonarivo et al. proposed a method to estimate the structural impedance matrix that uses the correlation of random noise, which was validated by a tank experiment [10, 11]. As the inverse of a structural impedance matrix, the structural-admittance matrix represents the normal velocity response on the surface of an object subjected to a normal point force. Its diagonal elements are the self-admittance, and the off-diagonal elements are the mutual admittance. From the perspective of operability, Williams et al. obtained the structural-admittance matrix of a spherical shell by using random sources in a non-anechoic room [12, 13].

Numerous works have been published about local impedance of underwater anechoic coatings [14], and

[1] The article is published in the original.

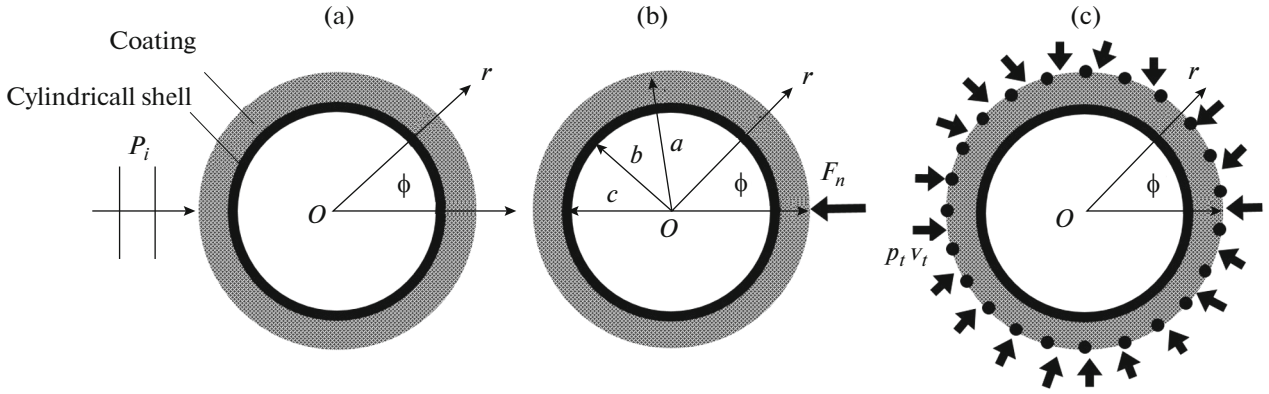

Fig. 1. Coated cylindrical shell excited by (a) a plane wave, (b) a normal point force, and (c) a random noise field.

such impedances are often measured in water-filled tubes [15–17]. Nevertheless, their non-local property is non-negligible and is of concern [18]. Faverjon et al. [19, 20] constructed an equivalent acoustic impedance model for a soundproofing scheme of a three-dimensional porous medium, and Yang et al. [21] further demonstrated that the non-local property of acoustic impedance strongly affects acoustic scattering, which means that mutual admittance is required to ensure that the scattered field is accurately computed.

Motivated by the results of Bobrovnitskiĭ and Williams, the present work investigates the characteristics of in vacuo structural admittance of infinite, coated cylindrical shells to lay the groundwork for the further research on the scattering of more complex coated objects. We derive analytical expressions of the structural admittance of a coated cylindrical shell for various external forces, and give numerical evaluations of the structural admittance. The scattered field is determined. An algebraic model and the approximation of the structural admittance are studied. Finally, conclusions are drawn and the main results are summarized.

ANALYTICAL EXPRESSION OF STRUCTRUAL ADMITTANCE

Analytical expressions of the structural admittance of a coated cylindrical shell are derived for various external forces: a plane acoustic wave, a normal point force, and a random noise field. The first two cases are used for theoretical analysis and the last one—for the simulation.

Firstly, consider a coated elastic cylindrical shell with a circular cross-section and a given incident plane wave of angular frequency ω propagating in the horizontal direction. A cylindrical coordinate system (r, ϕ) is adopted in the model, as shown in Fig. 1a. The interior of the shell is a vacuum. The external radius of the coating and the external and inner radii of the shell are denoted a, b, and c, respectively. The coating and the shell labeled 1 and 2, respectively, are described by the densities ρ_i, Young's modulus E_i and Poisson's ratio v_i. The exterior fluid is described by the density ρ_0, sound velocity c_0, and wave number $k_0 = \omega_0/c_0$. The time dependence $e^{j\omega t}$ is not explicitly written.

In the outer medium, the incident plane wave is written as

$$p_i = \sum_{n=-\infty}^{\infty} j^n J_n(k_0 r)\exp(jn\phi). \quad (1)$$

The scattered field is written as

$$p_s = \sum_{n=-\infty}^{\infty} j^n R_n H_n^{(1)}(k_0 r)\exp(jn\phi), \quad (2)$$

where the functions J_n and $H_n^{(1)}$ refer to the Bessel function and the Hankel function of the first kind of order n, respectively. R_n is the scattering coefficient of the structure.

According to elasticity theory [22, 23], the elastic waves in the solid can be expressed by the displacement potentials φ_i and ψ_i as follows:

$$\varphi_i = \sum_{n=-\infty}^{\infty} j^n \left[a_{ni} J_n(k_{li} r) + b_{ni} Y_n(k_{li} r)\right]\exp(jn\phi), \quad (3a)$$

$$\psi_i = \sum_{n=-\infty}^{\infty} j^n \left[c_{ni} J_n(k_{si} r) + d_{ni} Y_n(k_{si} r)\right]\exp(jn\phi), \quad (3b)$$

where the function Y_n refers to the Neumann function, (k_{li}, k_{si}) are the wave numbers of the compression and shear waves in the coating and shell, and (a_i, b_i, c_i, d_i) are the modal coefficients.

Then, R_n is determined from the boundary conditions [23]. The reader can refer to the literatures [10, 23] for the detailed derivations. The analytical solution of the scattered field is determined by Eq. (2). The

normal velocity on the external surface follows from Euler's equation:

$$v_1(a,\phi) = \frac{1}{j\rho_0 c_0}\sum_{n=-\infty}^{\infty} j^n\left[J_n'(k_0a) + R_nH_n^{(1)'}(k_0a)\right]\exp(jn\phi). \quad (4)$$

According to the impedance theory of sound scattering [1, 10], the modal coefficients of the structural admittance are calculated as follows:

$$y_{sn}(a) = -\frac{v_n(a)}{p_n(a)} = \frac{j}{\rho_0 c_0}\frac{J_n'(k_0a) + R_nH_n^{(1)'}(k_0a)}{J_n(k_0a) + R_nH_n^{(1)}(k_0a)}, \quad (5)$$

which are the reciprocal of the modal coefficients of the structural impedance (see Eq. (11) in [10]). The structural admittance is independent of the exterior fluid medium and may be obtained in a random noise field.

The structural admittance is calculated from the modal coefficients in Eq. (5) by using the inverse Fourier transform:

$$Y_s(\phi) = \sum_{n=-\infty}^{\infty} y_{sn}(a)\exp(jn\phi). \quad (6)$$

Therefore, the relationship between the total pressure and the normal velocity on the surface satisfies

$$\mathbf{v}_1 = -\mathbf{Y}_s\mathbf{p}_1. \quad (7)$$

Secondly, as the inverse of the structural impedance matrix, the structural-admittance matrix represents the normal velocity response on the surface of an object subjected to a normal point force. Its diagonal elements are the self-admittance, and the off-diagonal elements are the mutual admittance. The analytical expression for the structural admittance can be derived for a single point excitation.

Consider the two-dimensional coated cylindrical shell excited by a normal point force, as shown in Fig. 1b. The point force located at $(a,0)$ can be written as

$$f_r = \sum_{n=-\infty}^{\infty} f_{rn}\exp(jn\phi). \quad (8)$$

Similarly, the coefficients (a_i,b_i,c_i,d_i) are also obtained from the boundary conditions. The normal velocity on the surface of the coating is

$$\begin{aligned} v_{r1}(a,\phi) &= -j\omega\left(\frac{\partial\varphi_1}{\partial r} + \frac{1}{r}\frac{\partial\psi_1}{\partial\phi}\right)\Big|_{r=a} \\ &= -j\omega\sum_{n=-\infty}^{\infty} j^n\left[k_{l1}a_{n1}J_n'(k_{l1}a)\right. \\ &\quad \left. + k_{l1}b_{n1}Y_n'(k_{l1}a)\right]\exp(jn\phi) \\ &\quad - j\omega\sum_{n=-\infty}^{\infty} j^n\left[\frac{1}{a}jnc_{n1}J_n(k_{s1}a)\right. \\ &\quad \left. + \frac{1}{a}jnd_{n1}Y_n(k_{s1}a)\right]\exp(jn\phi). \end{aligned} \quad (9)$$

The structural admittance is

$$Y_s(\phi) = \frac{v_{r1}(\phi)}{f_r}. \quad (10)$$

After a few manipulations, it is easy to see that Eqs. (6) and (10) are the same, which shows that the structural admittance is independent of the exterior medium and fluid loading.

Finally, an encompassing and spatially random noise field is simulated by using the finite-element software COMSOL Multiphysics [10, 12], whose schematic diagram is shown in Fig. 1c. Taking the pressure and normal velocity on the external surface of coating, the cross-correlation matrices are obtained by the average of L realizations $\mathbf{p}_1,\ldots,\mathbf{p}_L$ [24]:

$$\langle\mathbf{v}\mathbf{v}^*\rangle = \frac{1}{L}\sum_{k=1}^{L}\mathbf{v}_k\mathbf{v}_k^*,\ \langle\mathbf{p}\mathbf{v}^*\rangle = \frac{1}{L}\sum_{k=1}^{L}\mathbf{p}_k\mathbf{v}_k^*, \quad (11)$$

where the superscript * stands for the conjugate transpose. The inverse of the factor $\mathbf{p}\mathbf{v}^*$ is then computed by using a singular value decomposition (SVD). In line with Eq. (7), the structural admittance is solved by [12]

$$\mathbf{Y}_s = \langle-\mathbf{v}\mathbf{v}^*\rangle\langle\mathbf{p}\mathbf{v}^*\rangle^{-1} \approx -\frac{1}{L}\sum_{k=1}^{L}\mathbf{v}_k\mathbf{v}_k^*\sum_{q=1}^{N_s}\frac{1}{\lambda_q}\mathbf{V}_q\mathbf{U}_q^*, \quad (12)$$

where we used the N_s eigenvalues $\lambda_q, q = 1,2,\ldots,N_s$ and column eigenvectors $\mathbf{U}_q$ and $\mathbf{V}_q$. A small eigenvalue may cause a calculation error. As opposed to the first two analytical methods, the method using the correlation of random noise can determine the structural admittance of an elastic object of arbitrary geometry.

NUMERICAL EVALUATIONS OF STRUCTURAL ADMITTANCE

The cylindrical shell has an outer radius $b = 0.5$ m, thickness $h_2 = 5$ mm, and the ratio $h_2/b = 1\%$. The coating has a thickness $h_1 = 5$ cm. The coating material is neoprene, which has a Young's modulus $E_1 = 4\times10^8$ Pa, a density $\rho_1 = 1300$ kg/m^3, and a Poisson's ratio $\sigma_1 = 0.49$ [25]. The cylindrical shell is steel with $E_2 = 210$ GPa, $\sigma_2 = 0.3$, and $\rho_2 = 7800$ kg/m^3, and the external fluid is water with $c_0 = 1500$ m/s and $\rho_0 = 1000$ kg/m^3.

Whether a point force or a plane wave, the exciting forces can be expanded into a Fourier series, and their structural admittances are the same. For a cylindrical shell, Fig. 2 displays the analytical drive-point admittance ($\phi = 0°$) and mutual admittance ($\phi = 180°$) versus frequency, which are compared with the numerical results obtained by FEM. The arc angle ϕ denotes the distance of mutual admittance between the drive point and the receiving point. An angle of 0° represents the driving-point admittance (or self-admittance).

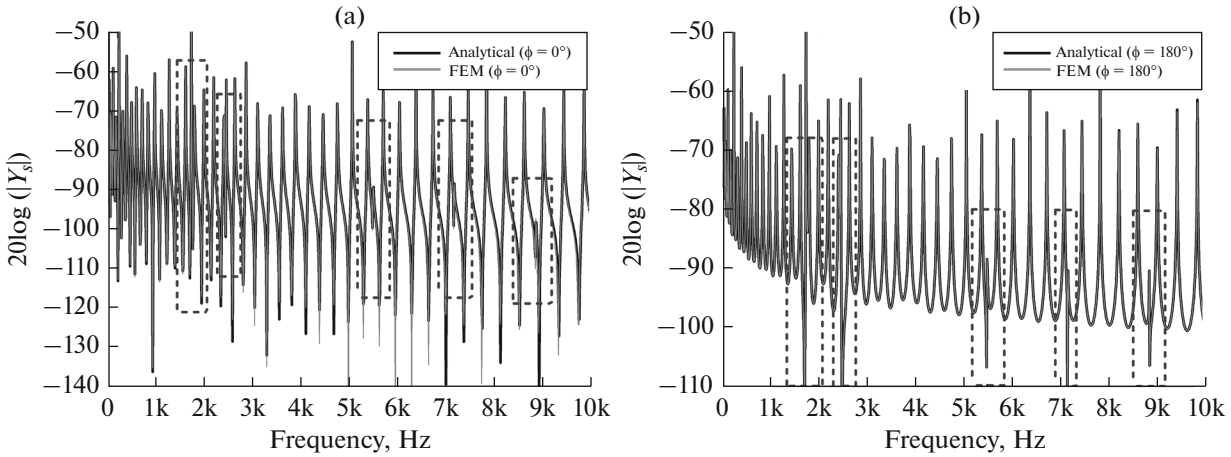

Fig. 2. Structural admittance of the coated cylindrical shell (a) at $\phi = 0°$ and (b) at $\phi = 180°$.

The analytical admittance is consistent with the numerical results, which verifies the analytical methods. The peaks are the resonance frequencies of the flexural modes on the shell, the width of which is related to the structural loss [12]. The wavelength at the resonance frequencies is related to the perimeter of the shell. In addition, some special peaks appear at 1740, 2461, 5502.5, 7174.3, and 8872.3 Hz. Figures 3b–3f show the magnitude of the displacements and deflection, and Fig. 3a shows the vibration at the common resonance frequency 1620 Hz. The common resonance in Fig. 3a is the high-order flexural resonance, whereas those in Figs. 3b–3f are low-order flexural resonance (zeroth to fifth order). The low-order modes have strong radiation efficiency at the resonance frequencies.

The structural admittance of uncoated and coated cylindrical shells as a function of frequency and arc angle are calculated analytically and shown in Fig. 4. The blue striped areas in Fig. 4 with smallest values, where the mutual admittance tends to zero, correspond to nodal areas on the shell, and the red areas with greatest values are the anti-nodal regions, which oscillate as a function of angle.

Some resonance modes of the cylindrical shell are shown in Fig. 3 and their resonance frequencies correspond to the peaks in Fig. 2. For a coated cylindrical shell, one striking difference is that the bright stripes are darker and the blue striped areas are broader, especially at high frequencies, which indicates that the magnitude of the structural admittance decreases. When the frequency is constant, the mutual admittance decreases with increasing arc distance, which indicates that the coating suppresses vibrations at high frequencies. In addition, a bright stripe appears at 1087 Hz. The structural displacements of coated cylindrical shell at 1087 Hz is similar to the resonance of the uncoated shell at 1740 Hz in Fig. 3b. This result shows that the equivalent shell mass increases because of the coating, so the resonance frequency redshifts. Similar phenomena occur at other low-order resonance frequencies, but are not obvious in Fig. 4b because the resonances are relatively weak.

In the simulated random noise field, the pressure and normal velocity on the structural surface are used to construct the matrices $\langle \mathbf{v}\mathbf{v}^* \rangle$ and $\langle \mathbf{p}\mathbf{v}^* \rangle$. To invert $\langle \mathbf{p}\mathbf{v}^* \rangle$ by using the truncated SVD of Eq. (12), we must carefully choose N_s, which is the number of singular values admitted at each frequency of interest [12]. Figure 6 gives the first 40 eigenvalues at 1 kHz.

The singular values follow the stair-step distributions and then fall into the computational noise after flat plateaus. The stair-step distributions are due to two kinds of modes ($-n$ and n) with the same magnitudes except for the zeroth-order mode. The magnitude of an eigenvalue represents the contribution of the mode corresponding to the structural vibration. In addition, the eigenvalues in air are greater and the flat plateaus are longer than in water, which means that the eigenvalues are more effective.

The random incident noise field is made of plane waves propagating in random directions. To illustrate the physical significance, Fig. 7 shows the modal decomposition of the surface velocity on the structure excited by a plane wave, which corresponds to the singular values in Fig. 6. On the one hand, two types of resonance frequencies are found for the modes in air (see Figs. 7a, 7c). The first type only has peaks and the second type has higher frequencies and includes peaks and valleys. In addition, the resonance frequencies of lower order modes are less than those of higher-order modes. Compared with the case for air, the magnitude of the structural normal velocity in water decreases as a whole. The first type of resonance frequencies also decreases and even disappears, whereas the second type remains almost unchanged (e.g., at 1740 Hz in Fig. 7a and at 980 Hz in Fig. 7c). Note that the max-

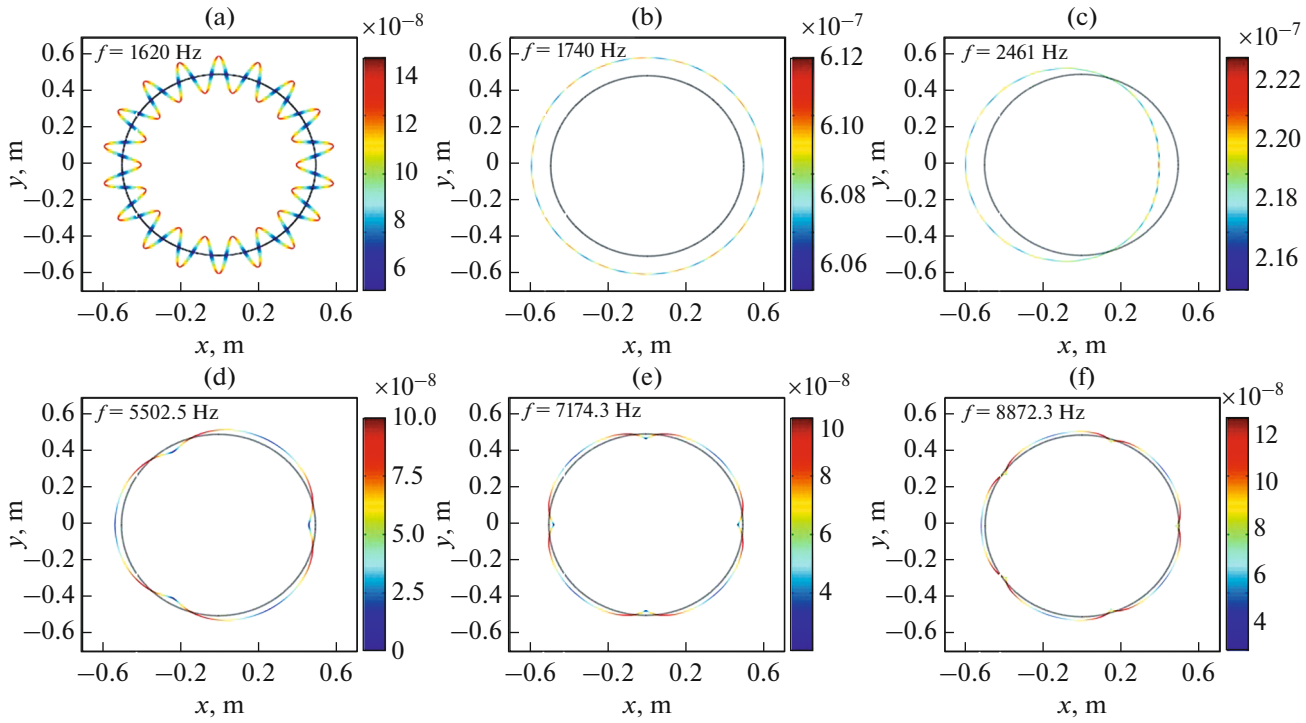

Fig. 3. Magnitude of structural displacement and deformation at resonance frequencies.

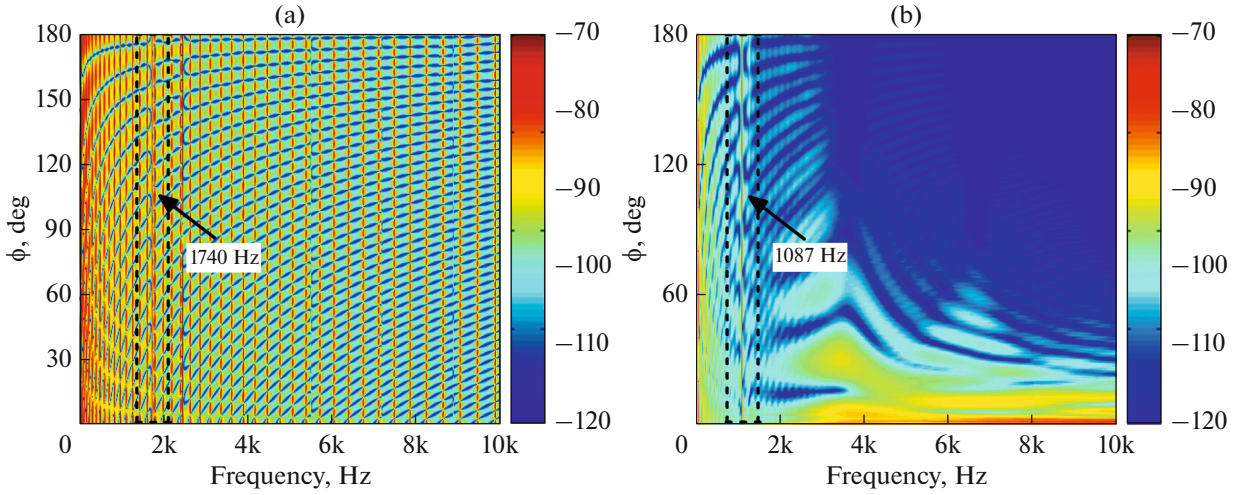

Fig. 4. Magnitude in dB of structural admittance versus frequency and arc angle of (a) a cylindrical shell and (b) a coated cylindrical shell.

ima of the second type are greatly reduced and even disappear (e.g., at 2460 Hz in Fig. 7a and at 1280 Hz in Fig. 3c). The fluid loading strongly affects the velocity at low frequencies. On the other hand, the magnitude of normal velocity of the coated cylindrical shell is less than that of the cylindrical shell. In addition, note that the singular values of the matrices $\langle \mathbf{pv}^* \rangle$ and $\langle \mathbf{vv}^* \rangle$ are the same, although this is not presented herein. Because of the loss of coating, the Bessel function with imaginary argument becomes incorrect at high frequencies (e.g., $ka > 80$).

For the sake of the image resolution in Fig. 7, not all efficient modes are given. To determine the cutoff value N_s for the SVD, Fig. 8 shows the Fourier coefficients of the decomposition versus modal order. The series can be truncated at a modal order $n = N_t$, which means that the mode orders $-N_t \sim N_t$ make the main contributions, whereas others modes are neglected.

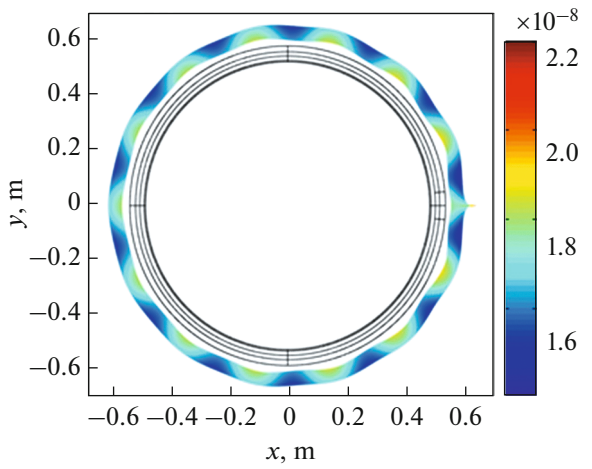

Fig. 5. Structural displacement and deformation of coated cylindrical shell at 1087 Hz.

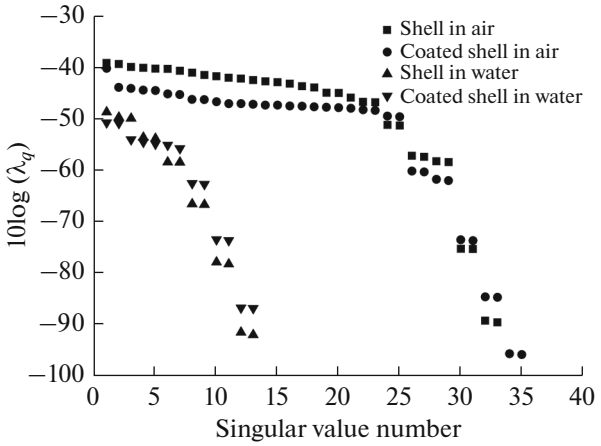

Fig. 6. Eigenvalues of matrix $\mathbf{pv}^*$ for uncoated and coated cylindrical shells at 1 kHz.

Thus, we can choose a dominant mode-based determination of $N_s = 2N_t + 1$ in Eq. (12). For the case of air at 1 kHz, it is reasonable to set $N_t = 15$, whereas $N_t = 5$ is chosen for water. There are more orders in air than in water, which illustrates that the singular values in air decrease more slowly. In addition, the magnitudes of the Fourier coefficients for the coated cylindrical shell are generally smaller than those of the cylindrical shell.

SCATTERED FIELD

According to the impedance theory of sound scattering, the structural, acoustic, and internal admittance are defined by

$$\mathbf{v}_i = -\mathbf{Y}_i \mathbf{p}_i, \tag{13a}$$

$$\mathbf{v}_s = \mathbf{Y}_a \mathbf{p}_s, \tag{13b}$$

$$\mathbf{v}_i + \mathbf{v}_s = -\mathbf{Y}_s (\mathbf{p}_i + \mathbf{p}_s), \tag{13c}$$

where $(\mathbf{p}_i, \mathbf{p}_s)$ denote the incident and scattered pressure column on the surface, respectively, and $(\mathbf{v}_i, \mathbf{v}_s)$ denote the corresponding velocity column. The admittance matrices $(\mathbf{Y}_i, \mathbf{Y}_s)$ depend only on the geometry of the exterior surface and on the properties of exterior fluid, which can be calculated by using the Green's function in free space [10, 13]. With these equations, we can write the surface scattered pressure as

$$\mathbf{p}_s = (\mathbf{Y}_a + \mathbf{Y}_s)^{-1} (\mathbf{Y}_i - \mathbf{Y}_s) \mathbf{p}_i. \tag{14}$$

In the previous section, we obtained the structural admittance of a coated cylindrical shell for three external forces: a normal point force, a plane wave, and a random noise field. Next, the scattered pressure on the structural surface in water is calculated by using Eq. (14) (see results in Fig. 9). Direct analytical solutions of Eq. (2) and numerical solutions obtained by FEM are also calculated for comparison, and both the real and imaginary parts of the scattered pressure are consistent with these results.

ALGEBRAIC MODEL AND APPROXIMATION OF STRUCTURAL ADMITTANCE

Due to the inverse relation, the characteristics of the structural-admittance matrix are similar to those of the usual admittance matrix. Both are symmetric matrices. For a coated structure, the mutual admittance Y_{ij} decreases with increasing surface distance r_{ij}. Y_{ij} approaches the self-admittance when r_{ij} tends to zero. According to Faverjon's model [19, 20], the algebraic model of structural admittance can be written as

$$Y_{ij} = |\zeta| \left[\rho_R (r_{ij}, \omega) \frac{\zeta_R}{|\zeta|} + j \rho_I (r_{ij}, \omega) \right], \tag{15}$$

where r_{ij} is the arc distance between the point i and j on the structural surface, and ζ denotes the local acoustic admittance given by Eq. (16). The quantities $\rho_R (r_{ij}, \omega)$ and $\rho_I (r_{ij}, \omega)$ are the real and imaginary parts of acoustic density functions, respectively:

$$\zeta = Y_n^{loc} = \frac{1}{N} \sum_{i=1}^{N} Y_{ii}, \tag{16}$$

$$\begin{cases} \rho_R (r_{ij}, \omega) = e^{-r_{ij}/L_R} \cos(2\pi r_{ij}/\lambda_R) \\ \rho_I (r_{ij}, \omega) = e^{-r_{ij}/L_I} \cos(2\pi r_{ij}/\lambda_I + \phi_I), \end{cases} \tag{17}$$

$$\cos(\phi_I(\omega)) = \zeta_I/\zeta(\omega), \phi_I(\omega) \in [0, \pi], \tag{18}$$

where N is the dimension of the matrix, (L_R, L_I) are the decay distances controlling the exponential damping of amplitude, (λ_R, λ_I) are the oscillation wavelengths, and ϕ_I is the phase shift. Therefore, the parameters have definite physical meanings and

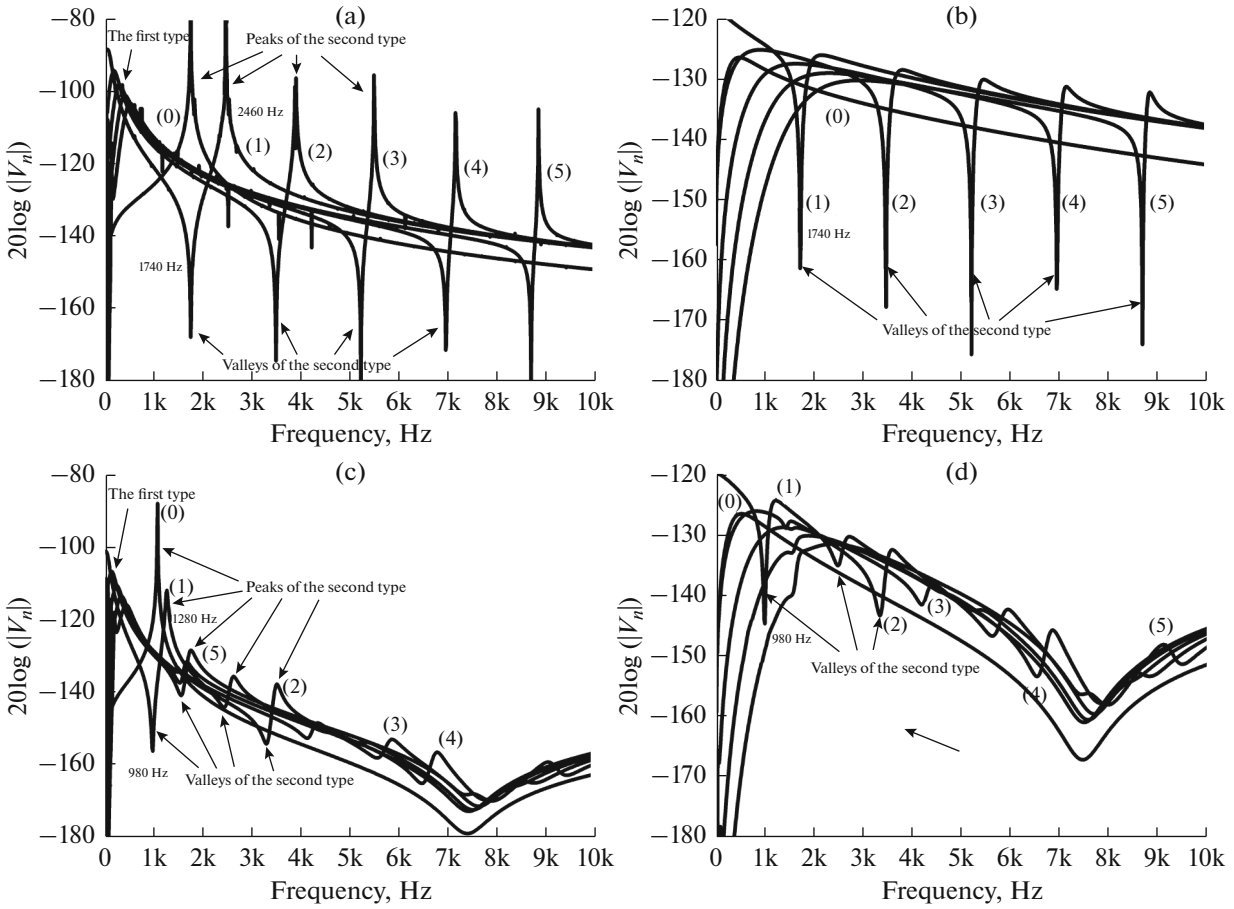

Fig. 7. Modal decompositions of surface velocity on structure excited by a plane wave for $n = 0...5$ computed from the analytic solution in Eq. (9). (a) Cylindrical shell in air; (b) cylindrical shell in water; (c) coated cylindrical shell in air; (d) coated cylindrical shell in water.

describe the distribution of elements in the structural-admittance matrix.

By using the software "Origin", the above parameters can be determined by fitting to a coated cylindrical shell. The table gives results at 2, 3, 5, and 7 kHz. The parameters λ_R and λ_I show a decreasing trend, which is consistent with the variation of mutual admittance. The fitted curves are compared with the density functions of mutual admittance at 5 kHz. They are basically consistent near the self-admittance, which makes a major contribution to the scattered field. The contribution of the mutual admittance to the scattered field decreases with increasing distance.

For the coated complex structure, the structural-admittance matrix is typically large and requires an intensive calculation. Thus, it is helpful to simplify the matrix. After the mutual admittance is truncated at the distance r_{ij}, a new structural-admittance matrix is constructed and the scattered pressure is recalculated by using Eq. (14). Taking 5 and 7 kHz as examples, the absolute errors between the approximated and exact scattered pressure are evaluated (see Fig. 11). The results are divided into four sections by $0 < r_{ij} < 0.125$ m, $0.125 < r_{ij} < 0.25$ m, and $0.25 < r_{ij} < 0.5$ m in Fig. 11. For the first interval of 0–0.125 m, the error fluctuates greatly in the range between 0 and 1, and so the mutual admittance strongly affects the scattered field. When

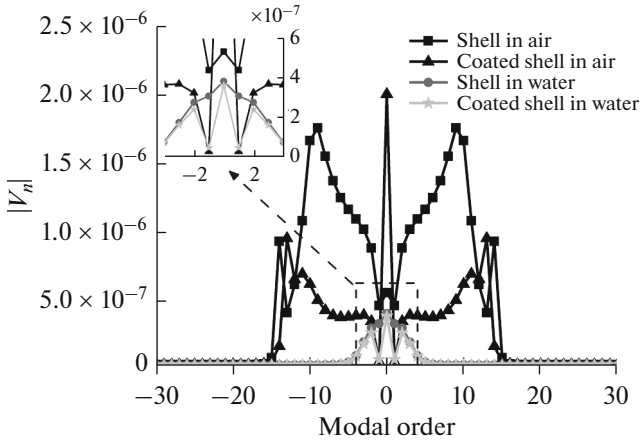

Fig. 8. Mode coefficient of normal velocity on the structural surface.

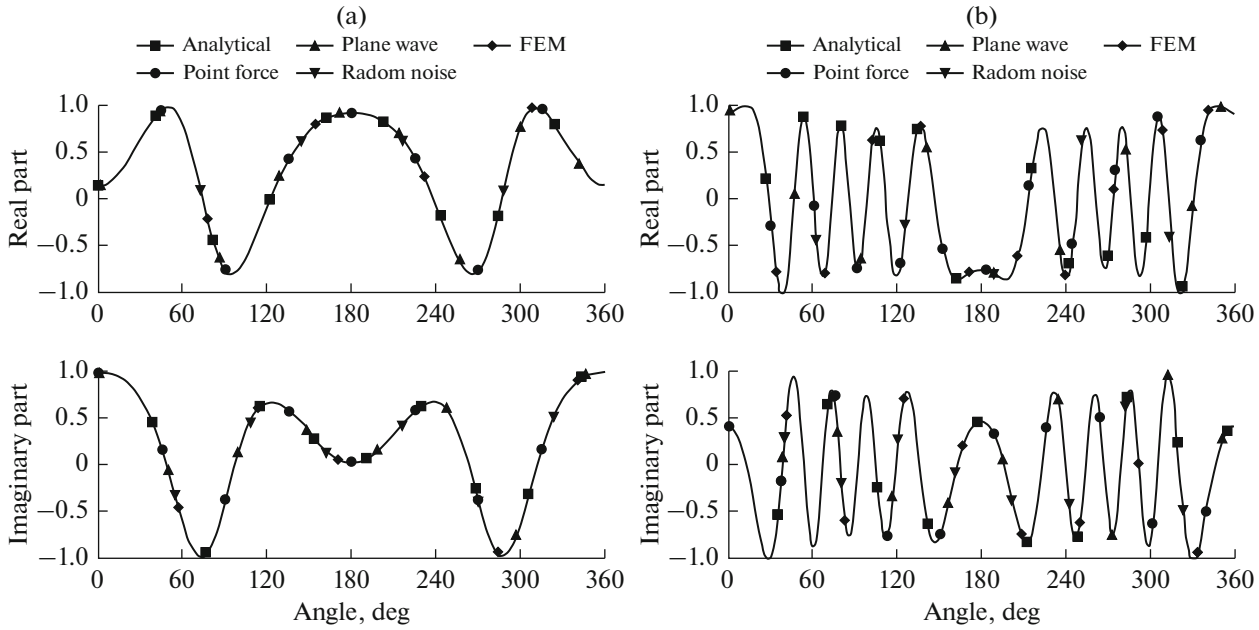

Fig. 9. Scattered field on the structural surface at (a) 2 and (b) 7 kHz.

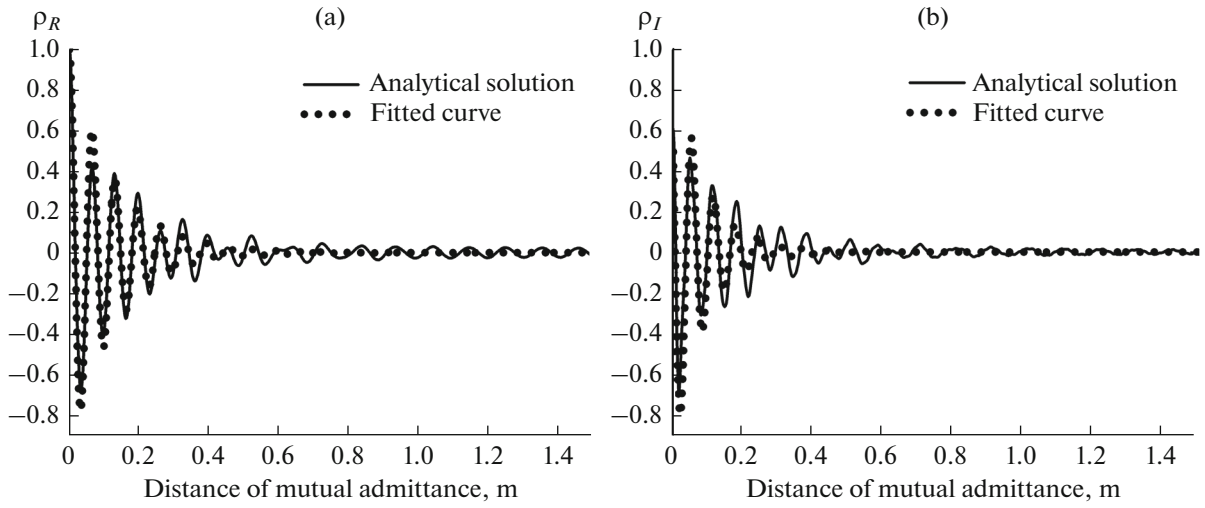

Fig. 10. (a) Real part ρ_R and (b) imaginary part ρ_I of the density function of structural admittance at 5 kHz.

the distance is 0.125–0.25 m, the error is 0–0.4. Subsequently, the error decreases exponentially. When the distance exceeds 0.5 m, the error is less than 0.1 and approaches zero, which means that the effect of the mutual admittance on the scattered field is almost negligible. For the frequencies of 5 and 7 kHz, the admittance can be regarded as "local" admittance in the range of 0–0.5 m, which behaves as a diagonal sparse matrix.

Table 1. Results for fitted parameters

Frequency, Hz	L_R	λ_R	L_I	λ_I	ϕ_I
2000	0.4236	0.1650	0.0578	0.1536	0.7021
3000	0.0779	0.1298	0.0536	0.1176	0.7324
5000	0.1288	0.0655	0.0884	0.0628	1.0603
7000	0.0568	0.0454	0.0413	0.0423	0.8377

CONCLUSIONS

The in vacuo structural admittance of an infinite, coated cylindrical shell is investigated theoretically and numerically. The analytical expressions of the structural admittance are derived for the cases of vari-

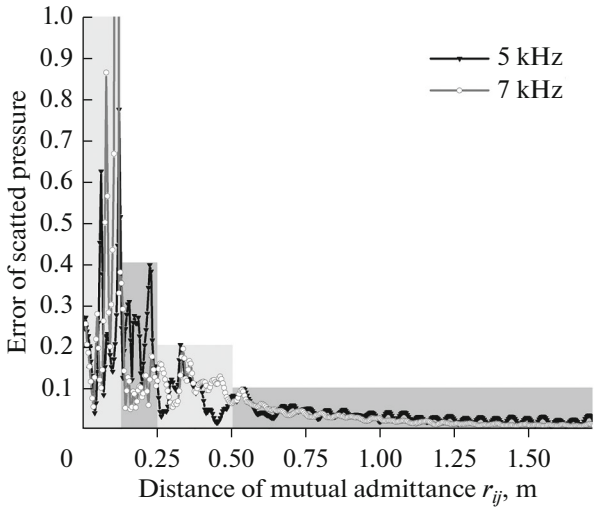

Fig. 11. Absolute error in scattered pressure at structural surface at 5 and 7 kHz.

ous external forces: a plane acoustic wave, a normal point force and a random noise field. The first two cases are used for theoretical analysis and the last case is simulated by FEM. The structural admittance is evaluated numerically. The results show that the structural admittance depends only on the object's structural parameters and is independent of the external medium and of fluid loading. According to the impedance theory of sound scattering, the scattered field of a coated cylindrical shell is calculated by combining the structural-, acoustic-, and internal-admittance matrices. The measuring method based on a simulated random noise field provides guidance for developing a measurement procedure to predict the scattered field of complex coated objects in any medium. Because of the non-local property of structural surface admittance, we study a local approximation of the structural admittance and build an algebraic model of the coated object by nonlinear curve fitting. Finally, the large matrices should be simplified to facilitate research on the structural vibration.

ACKNOWLEDGMENTS

The study was supported by the National Basic Research Program of China (973 Program), project no. 613247.

REFERENCES

1. Yu. I. Bobrovnitskii, Acoust. Phys. **52**, 513 (2006).
2. Yu. I. Bobrovnitskii, J. Sound Vib. **297**, 743 (2006).
3. C. Langrenne, M. Melon, and A. Garcia, J. Acoust. Soc. Am. **121**, 2750 (2007).
4. E. G. Williams, *Fourier Acoustics: Sound Radiation and Nearfield Acoustical Holography* (Academic Press, 1999).
5. M. Zampolli, F. B. Jensen, and A. Tesei, J. Acoust. Soc. Am. **125**, 89 (2009).
6. Yu. I. Bobrovnitskii, Acoust. Phys. **52**, 638 (2006).
7. Yu. I. Bobrovnitskii, Acoust. Phys. **53**, 535 (2007).
8. Yu. I. Bobrovnitskii, K. D. Morozov, and T. M. Tomilina, Acoust. Phys. **56**, 127 (2010).
9. C. F. Gaumond and T. Yoder, J. Acoust. Soc. Am. **97**, 1415 (1995).
10. S. T. Rakotonarivo, W. A. Kuperman, and E. G. Williams, J. Acoust. Soc. Am. **134**, 4401 (2013).
11. S. Rakotonarivo, S. Yildiz, P. Roux, E. G. Williams, and W. A. Kuperman, in *Proc. 2nd Int. Conference on Underwater Acoustics* (Island of Rhodes, 2014).
12. E. G. Williams, J. D. Tippmann, S. T. Rakotonarivo, Z. J. Waters, P. Roux, and W. A. Kuperman, J. Acoust. Soc. Am. **142**, 103 (2007).
13. J. D. Tippmann, S. T. Rakotonarivo, W. Kuperman, Z. J. Waters, P. Roux, and E. G. Williams, in *Proc. 22nd Int. Congress on Acoustics, ICA 2016* (Buenos Aires, September 5–9, 2016).
14. E. Brandão, A. Lenzi, and S. Paul, Acta Acust. Acust. **101**, 443 (2015).
15. J. Y. Chung and D. A. Blaser, J. Acoust. Soc. Am. **68**, 907 (1980).
16. J. Y. Chung and D. A. Blaser, J. Acoust. Soc. Am. **68**, 914 (1980).
17. E. J. Skudrzyk, J. Acoust. Soc. Am. **74**, S109 (1983).
18. E. Brandão, P. Mareze, A. Lenzi, and A. R. da Silva, J. Acoust. Soc. Am. **133**, 2722 (2013).
19. B. Faverjon and C. Soize, J. Sound Vib. **276**, 571 (2004).
20. B. Faverjon and C. Soize, J. Sound Vib. **276**, 593 (2004).
21. M. Yang, T. Wang, Z. Fan, and Z. Jin, in *Proc. 16th AIAA/CEAS Aeroacoustics Conference* (Stockholm, 2010), p. 3907.
22. M. C. Junger and D. Feit, *Sound, Structures, and their Interaction* (MIT Press, Cambridge, 1986).
23. R. D. Doolittle and H. Überall, J. Acoust. Soc. Am. **39**, 272 (1996).
24. W. A. Kuperman and F. Ingenito, J. Acoust. Soc. Am. **67**, 1988 (1980).
25. W. Tang, S. He, and J. Fan, Acta Acust. (Beijing) **30**, 289 (2005).